Synthesis of Point Planar Elastic Behaviors Using Three-Joint Serial Mechanisms of Specified Construction

Shuguang Huang[1]
Department of Mechanical Engineering,
Marquette University,
Milwaukee, WI 53201-1881
e-mail: huangs@marquette.edu

Joseph M. Schimmels
Department of Mechanical Engineering,
Marquette University,
Milwaukee, WI 53201-1881
e-mail: j.schimmels@marquette.edu

This paper presents methods for the realization of 2×2 translational compliance matrices using serial mechanisms having three joints, each either revolute or prismatic and each with selectable compliance. The geometry of the mechanism and the location of the compliance frame relative to the mechanism base are each arbitrary but specified. Necessary and sufficient conditions for the realization of a given compliance with a given mechanism are obtained. We show that, for an appropriately constructed serial mechanism having at least one revolute joint, any single 2×2 compliance matrix can be realized by properly choosing the joint compliances and the mechanism configuration. For each type of three-joint combination, requirements on the redundant mechanism geometry are identified for the realization of every point planar elastic behavior at a given location, just by changing the mechanism configuration and the joint compliances.
[DOI: 10.1115/1.4035189]

Keywords: compliance and stiffness realization, compliant mechanism, compliant behavior synthesis

1 Introduction

Passive compliance in actuation allows robots to achieve improved dexterity in manipulation and improved energy economy in walking and running [1,2]. Several strategies exist for achieving passive compliance actuation in a mechanism. Series elastic actuators (SEAs) [3] can be used to provide a selected amount of compliance in each joint. Variable stiffness actuators (VSAs) [4] are similar, but they allow joint compliance to be changed.

The space of compliant behaviors that can be achieved at a given location by a mechanism driven by SEAs corresponds to a single point; whereas, the space of behaviors that can be achieved by a mechanism driven by VSAs corresponds to a polyhedral convex cone for which the cone edges are determined by the mechanism kinematics. If the manipulator is kinematically redundant, an even larger set of compliances can be attained by both adjusting the joint stiffnesses and the manipulator configuration without ever changing the endpoint location of the robot.

Many robot tasks, such as opening a door or turning a crank, require motion and compliance in a single plane. In these tasks, the interaction force is important, and the interaction torque is not. Since only the relationship between force and translation is important, the interaction can be modeled as point contact, and the compliant behavior can be modeled as an elastically suspended particle, i.e., not an elastically suspended rigid body. This paper presents methods for the evaluation and realization of planar translational elastic behaviors (2×2 compliance matrices) using redundant serial mechanisms having three joints. Each joint is either revolute or prismatic, and each has selectable compliance. One of eight types of three-joint selectable-compliance planar mechanisms (RPR) is illustrated in Fig. 1. The mechanisms considered are arbitrary but have known link lengths.

1.1 Related Work. Spatial linear elastic behavior is represented by a 6×6 symmetric stiffness matrix $\mathbf{K}$ or compliance matrix $\mathbf{C}$. In previous work, screw theory [5–9] and Lie groups [10] have been used to analyze spatial linear elastic behavior.

In recent work, the realization of spatial elastic behavior through the design of passive compliant mechanisms has been addressed. Previously, the limitations of simple parallel mechanisms [11] and simple serial mechanisms [12] in realizing elastic behaviors have been identified. Synthesis procedures to achieve any elastic behavior within the simple-mechanism realizable subspace (subspace associated with mechanisms having no helical joints) have been developed [11–14]. Synthesis procedures to realize an *arbitrary* spatial stiffness matrix with a more complicated (helical joint) parallel or serial system have also been developed [15–19].

In more recent work [20], the realization of compliance in Euclidian space $E(2)$ using 3R serial mechanisms with known link lengths was addressed. Optimization was used to identify the mechanism configuration and joint stiffnesses that may or may not realize the targeted stiffness matrix. In other recent work [21–23], the synthesis of isotropic compliance in $E(2)$ and $E(3)$ with serial mechanisms has been addressed. These approaches do not guarantee a physical solution, and geometric conditions on mechanisms to ensure solution existence were not identified.

In our most recent work [24], realization of an arbitrary compliance in $E(2)$ with a serial mechanism having only revolute joints was addressed. Conditions for the realization of a given compliance with a given mechanism were identified. These realization conditions were then interpreted in terms of the geometric

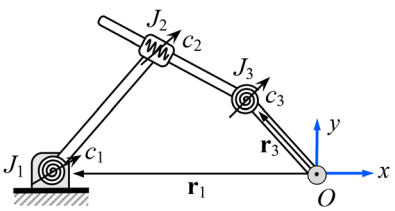

Fig. 1 One type of serial compliant mechanism (RPR) with variable stiffness actuators

[1]Corresponding author.

Manuscript received April 28, 2016; final manuscript received November 1, 2016; published online December 2, 2016. Assoc. Editor: Yuefa Fang.

relationships among the mechanism joint locations. The evaluation of the ability of a single mechanism to realize all compliances in $E(2)$ was also presented. The results developed in Ref. [24], however, cannot be applied directly to a mechanism that contains one or more prismatic joints. This is due to the fact that, unlike a revolute joint, the joint twist of a prismatic joint cannot be determined by the joint location alone. Methods and theory for the realization of an arbitrary compliance with a *general* serial mechanism having a specified construction are needed.

This work is motivated by the unresolved needs in compliance realization including: (1) the ability to identify the space of realizable compliances that can be achieved with a mechanism of specified geometry; (2) the ability to select the appropriate physical parameters so that a specified mechanism is able to achieve an arbitrary compliance within the realizable space; and (3) the ability to characterize mechanism geometries that will allow all realizable compliances to be achieved at a specified endpoint. These needs were discussed in Ref. [25] but not solved and were addressed in Ref. [24] but solved only for 3R planar mechanisms. This paper addresses these needs for planar translational elastic behavior realized using all of the other serial planar three-joint kinematic topologies.

1.2 Technical Background. Consider a planar serial mechanism having n joints (prismatic or revolute), J_i, with joint compliance c_i and joint twists $\mathbf{t}_i$. Then, the compliance matrix at the mechanism endpoint [26] is

$$\mathbf{C} = c_1\mathbf{t}_1\mathbf{t}_1^{\mathrm{T}} + c_2\mathbf{t}_2\mathbf{t}_2^{\mathrm{T}} + \cdots + c_n\mathbf{t}_n\mathbf{t}_n^{\mathrm{T}} \tag{1}$$

where the twists $\mathbf{t}_i$ are described relative to the compliance frame (the reference frame where the compliance matrix is specified). Each compliant joint provides a rank-1 symmetric positive semidefinite (PSD) component

$$\mathbf{C}_i = c_i\mathbf{t}_i\mathbf{t}_i^{\mathrm{T}} \tag{2}$$

For a suspended particle in planar motion, the compliance is a 2×2 PSD matrix. Each twist $\mathbf{t}_i$ is a two-vector.

For a prismatic joint J_i, the joint twist $\mathbf{t}_i$ is a unit vector along the prismatic joint axis, as shown in Fig. 2(*a*). If prismatic joint J_i is attached to the base or to any link that cannot rotate, $\mathbf{t}_i$ is constant. Thus, when considering the elastic properties of a prismatic joint, only the orientation of the joint is important; its two-vector twist used in calculating the joint compliance is independent of its location in space.

Unlike a prismatic joint, the elastic properties of a revolute joint depend on the joint location in space. The joint twist of a revolute joint is given as

$$\mathbf{t}_i = \mathbf{r}_i \times \mathbf{k}$$

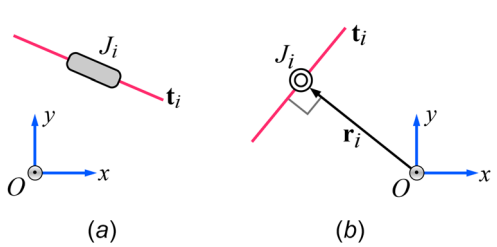

Fig. 2 Joint twists in a serial mechanism. (*a*) For a prismatic joint, the joint twist $\mathbf{t}_i$ is a unit vector along the prismatic joint axis. It is independent of the location of the joint. (*b*) For a revolute joint, the joint twist $\mathbf{t}_i$ is orthogonal to the position vector $\mathbf{r}_i$ and depends on the location of the joint.

where $\mathbf{r}_i$ is the position vector from the location of the compliance frame O to the location of joint i, as shown in Fig. 2(*b*), and $\mathbf{k}$ is the unit vector perpendicular to the plane.

For a revolute joint, the joint twist $\mathbf{t}_i$ can be obtained by rotating vector $\mathbf{r}_i$ either clockwise or counterclockwise about the coordinate frame origin. This is expressed as

$$\mathbf{t}_i = \pm\Omega\mathbf{r}_i \tag{3}$$

where Ω is the 2×2 antisymmetric matrix associated with a vector cross-product, given as

$$\Omega = \begin{bmatrix} 0 & 1 \\ -1 & 0 \end{bmatrix} \tag{4}$$

To realize a given compliance $\mathbf{C}$ with a given mechanism, the mechanism configuration ($\mathbf{t}_i$ values) and the joint compliances (c_i values) need to be determined so that Eq. (1) is satisfied.

1.3 Compliance Realization With 3R Mechanisms. The previously identified unresolved compliance realization needs for point planar elastic behavior have been addressed and solved for 3R mechanisms having variable stiffness joints [24]. The main results of Ref. [24] are summarized as:

(1) Limits on the space of elastic behaviors that can be realized with a 2R mechanism were identified.
(2) Necessary and sufficient conditions for the realization of a given compliance at a given configuration were identified and illustrated in terms of 3R mechanism geometry.
(3) Conditions used to assess the ability of a 3R mechanism to realize all compliant behaviors at a specific endpoint were identified.

Since joint twists $\mathbf{t}_i$ for revolute joints can be expressed in terms of joint position $\mathbf{r}_i$ (using Eq. (3)), realization conditions were described using the compliance $\mathbf{C}$ and each joint location $\mathbf{r}_i$. The joint twist of a prismatic joint, however, is independent of its position $\mathbf{r}_i$. Therefore, the results obtained for 3R mechanisms cannot be used directly for other types of three-joint mechanisms. A new but equivalent way to describe these results without using joint position vectors $\mathbf{r}_i$ is needed.

1.4 Overview. This paper presents means to analyze and realize planar translational elastic behaviors using three-joint serial mechanisms. The means for analysis and synthesis are based on the geometry of compliance matrix space and the geometry of the mechanism. The ability of a *single* mechanism with specified link lengths to realize *all* compliance behaviors is also investigated.

In Sec. 2, the results obtained for 3R serial mechanisms are extended to general three-joint serial mechanisms. In Secs. 3 and 4, the theories developed in Sec. 2 are applied to all types of three-joint mechanisms having prismatic and revolute joints. For each case, necessary and sufficient conditions for the realization of all elastic behaviors at a given location are obtained. General synthesis procedures to achieve a realizable compliance are presented in Sec. 5. A numerical example illustrating the synthesis procedures for a given mechanism is provided in Sec. 6. Finally, a brief summary is presented in Sec. 7.

2 Serial Planar Mechanism Compliance Realization

In this section, the theories obtained for 3R mechanisms [24] are generalized for three-joint mechanisms having either revolute or prismatic joints. For all mechanism types, joint twists (rather than joint locations) are used in the realization conditions.

First, the limitations of a two-joint mechanism in realizing an arbitrary compliance are described in terms of joint twists. Then, the realization of a given compliance with a general three-joint mechanism is addressed.

2.1 Limits of Mechanisms With Two Joints. In Ref. [24], the limitations of a 2R mechanism in realizing a specific compliance were identified. It was shown that a compliance matrix $\mathbf{C}$ can be realized with a 2R mechanism having joint locations $\mathbf{r}_1$ and $\mathbf{r}_2$ if and only if

$$\mathbf{r}_1^{\mathrm{T}}\mathbf{C}\mathbf{r}_2 = 0 \tag{5}$$

This condition can be expressed in terms of joint twists using Eq. (3). The more general equivalent expression for a two-joint mechanism having revolute or prismatic joints is given by:

PROPOSITION 1. *A compliance matrix* $\mathbf{C}$ *can be realized with a two-joint mechanism at a given configuration if and only if*

$$\mathbf{t}_1^{\mathrm{T}}(\Omega^{\mathrm{T}}\mathbf{C}\Omega)\mathbf{t}_2 = 0 \quad \text{or} \quad \mathbf{t}_1^{\mathrm{T}}\mathbf{K}\mathbf{t}_2 = 0 \tag{6}$$

where $\mathbf{t}_1$ *and* $\mathbf{t}_2$ *are the two joint twists at the given configuration, and* $\mathbf{K} = \mathbf{C}^{-1}$ *is the stiffness matrix.*

Note that the matrix $\Omega^{\mathrm{T}}\mathbf{C}\Omega$ in the first equation of Eq. (6) can be replaced with $\mathbf{K}$ for the full rank point planar case because

$$\Omega^{\mathrm{T}}\mathbf{C}\Omega = \det(\mathbf{C})\mathbf{C}^{-1} = \det(\mathbf{C})\mathbf{K} \tag{7}$$

The restriction on the space of realizable elastic behaviors can be described in terms of the mechanism geometry, as illustrated in Fig. 3. For a given location of the compliance frame, the position of joint J_1 relative to point O is specified, therefore, $\mathbf{t}_1$ is constant. By condition (6), joint twist $\mathbf{t}_2$ must be perpendicular to vector $\mathbf{K}\mathbf{t}_1$.

If l_1 is the straight line passing through O that is perpendicular to $\mathbf{K}\mathbf{t}_1$, condition (6) requires that joint twist $\mathbf{t}_2$ lies along line l_1. Thus, if J_2 is a prismatic joint, the joint axis must be along l_1; if J_2 is a revolute joint, it must be positioned such that $\mathbf{r}_2 \perp l_1$ at the compliance frame (or $\mathbf{r}_2$ lie along $\mathbf{K}\mathbf{t}_1$).

Due to this very limiting restriction on the configuration of a two-joint mechanism needed to realize a specified compliance, serial mechanisms having at least three joints must be considered.

2.2 Mechanisms With Three Compliant Joints. For a three-joint mechanism, since the degree-of-freedom is increased, the mechanism configuration is no longer fixed when the position of the suspended particle relative to the mechanism base is specified.

A necessary and sufficient condition for a 3R mechanism to realize $\mathbf{C}$ is provided in Ref. [24]. The condition expressed in terms of joint locations $\boldsymbol{r}_i$ can be equivalently expressed in terms of joint twists $\boldsymbol{t}_i$ and thus applies to a general three-joint mechanism. The generalized condition is:

PROPOSITION 2. *A compliance* $\mathbf{C}$ *can be realized with a three-joint mechanism with joint twists* $\mathbf{t}_1$, $\mathbf{t}_2$, *and* $\mathbf{t}_3$ *if and only if any two of the following inequalities hold:*

$$(\mathbf{t}_1^{\mathrm{T}}\Omega\mathbf{t}_2\mathbf{t}_2^{\mathrm{T}}\mathbf{K}\mathbf{t}_1)(\mathbf{t}_1^{\mathrm{T}}\Omega\mathbf{t}_3\mathbf{t}_3^{\mathrm{T}}\mathbf{K}\mathbf{t}_1) \le 0 \tag{8}$$

$$(\mathbf{t}_2^{\mathrm{T}}\Omega\mathbf{t}_3\mathbf{t}_3^{\mathrm{T}}\mathbf{K}\mathbf{t}_2)(\mathbf{t}_2^{\mathrm{T}}\Omega\mathbf{t}_1\mathbf{t}_1^{\mathrm{T}}\mathbf{K}\mathbf{t}_2) \le 0 \tag{9}$$

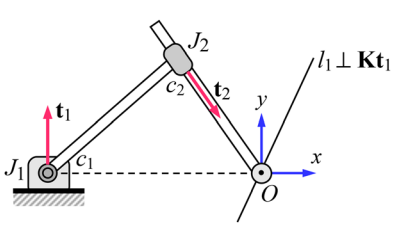

Fig. 3 Realization of a given compliance with a two-joint mechanism having a specified configuration. Joint twist $\mathbf{t}_2$ of J_2 must be collinear with line $l_1 \perp \mathbf{K}\mathbf{t}_1$ at point O to realize the given $\mathbf{C}$.

$$(\mathbf{t}_3^{\mathrm{T}}\Omega\mathbf{t}_1\mathbf{t}_1^{\mathrm{T}}\mathbf{K}\mathbf{t}_3)(\mathbf{t}_3^{\mathrm{T}}\Omega\mathbf{t}_2\mathbf{t}_2^{\mathrm{T}}\mathbf{K}\mathbf{t}_3) \le 0 \tag{10}$$

These conditions ensure that the specified compliance lies within the space of realizable compliant behaviors for a given mechanism configuration. The realizable space is spanned by the edges of a polyhedral convex cone determined by joint kinematics ($\mathbf{t}_i\mathbf{t}_i^{\mathrm{T}}$).

Similar to the 3R case [24], the mathematical conditions (8)–(10) can be geometrically described in the 2D plane of the mechanism.

Consider two lines l_1 and l_2 passing through the origin O (location of the suspended particle) and defined by $l_1 \perp \mathbf{K}\mathbf{t}_1$ and $l_2 \perp \mathbf{K}\mathbf{t}_2$. The two lines separate the plane into four zones: Z_1, Z_2, Z_3, and Z_4 as illustrated in Fig. 4(a).

If we denote

$$\Lambda_1 = Z_1 \cup Z_3, \quad \Lambda_2 = Z_2 \cup Z_4 \tag{11}$$

then, $\mathbf{t}_3$ must be either in Λ_1 or in Λ_2. Thus, once the twists associated with J_1 and J_2 are specified, either Λ_1 or Λ_2 is the acceptable space for the joint twist $\mathbf{t}_3$ of J_3. Since neither $\mathbf{t}_1$ nor $\mathbf{t}_2$ can be in the interior of the space acceptable for $\mathbf{t}_3$ (equivalent condition for $\boldsymbol{r}_i$ proved in Ref. [24]), the acceptable space is the one that does not contain $\mathbf{t}_1$ or $\mathbf{t}_2$ (illustrated in Fig. 4(a)).

If the mechanism kinematic topology and configuration are specified, the three joint twists are determined. The three unsigned joint twist directions $\mathbf{t}_1$, $\mathbf{t}_2$, and $\mathbf{t}_3$ divide the plane into six areas, S_{ij}, as illustrated in Fig. 4(b) with different shading. If we define

$$\Gamma_{12} = S_{12} \cup S_{21}, \Gamma_{13} = S_{13} \cup S_{31}, \Gamma_{23} = S_{23} \cup S_{32}$$

then, Γ_{ij} represents the two areas between the two lines associated with $\boldsymbol{t}_i$ and $\boldsymbol{t}_j$ as shown in Fig. 4(b). Similar to the 3R case [24], the realizability of compliance $\mathbf{C}$ is characterized by the relationships among the three twist action lines and the three lines l_i defined by $l_i \perp \mathbf{K}\mathbf{t}_i$ ($i = 1, 2, 3$). It can be proved that $\mathbf{C}$ can be realized with the mechanism at the given configuration if and only if: $\mathbf{t}_1$ is between and adjacent to lines l_2 and l_3; $\mathbf{t}_2$ is between and adjacent to lines l_1 and l_3; and $\mathbf{t}_3$ is between and adjacent to lines l_1 and l_2 as shown in Fig. 4(b).

In summary, we have:

PROPOSITION 3. *For a given compliance matrix* $\mathbf{C}$ *and a planar serial mechanism having three joints,*

(a) *If the two twists* $\mathbf{t}_1$ *and* $\mathbf{t}_2$ *are specified, the space of locations for* $\mathbf{t}_3$ *that allow realization of* $\mathbf{C}$ *is in the zone (*Λ_1 *or* Λ_2*) that does not contain* $\mathbf{t}_1$ *or* $\mathbf{t}_2$ as shown in Fig. 4(a).

(b) *If the three twists* $\mathbf{t}_1$, $\mathbf{t}_2$, *and* $\mathbf{t}_3$ *are specified,* $\mathbf{C}$ *can be realized if and only if*

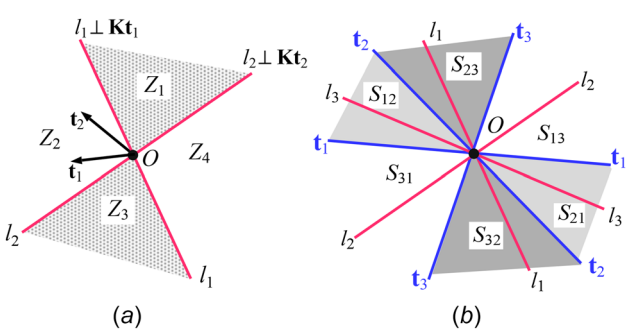

Fig. 4 Relationship between joint twists $\mathbf{t}_i$ and lines l_i. (*a*) If two joints are specified, the acceptable area for $\mathbf{t}_3$ is determined by lines l_1 and l_2. (*b*) Realization condition: $\mathbf{t}_1$ must be between and adjacent to lines l_2 and l_3; $\mathbf{t}_2$ must be between and adjacent to lines l_1 and l_3; and $\mathbf{t}_3$ must be between and adjacent to lines l_1 and l_2.

$$l_1 \in \Gamma_{23}, \quad l_2 \in \Gamma_{13}, \quad l_3 \in \Gamma_{12} \tag{12}$$

as shown in Fig. 4(b).

Similar to conditions (8)–(10), the three conditions in Eq. (12) are not independent. If any two conditions in Eq. (12) are true, the remaining condition must also be true.

2.3 Kinematic Compliance Realization Conditions. The entire space of compliances that are realizable with a mechanism is the union of realizable spaces associated with all possible configurations. In Ref. [24], realization conditions for 3R mechanisms were obtained in terms of joint locations $\mathbf{r}_i$. When the compliance frame relative to the mechanism base J_1 is specified, the ability of a 3R mechanism to realize all compliances depends on the ranges in joint locations that $\mathbf{r}_2$ and $\mathbf{r}_3$ can have while maintaining the endpoint position.

Similarly, for a general three-joint mechanism, when the position of the endpoint O relative to the mechanism base J_1 is specified, the twist $\mathbf{t}_1$ is constant whether it is prismatic or revolute. Thus, when the mechanism changes its configuration with a specified endpoint O, the joint twists $\mathbf{t}_2$ and $\mathbf{t}_3$ change and span two spaces. The ability of a mechanism to realize an arbitrary compliance depends on the two twist spaces.

PROPOSITION 4. *Consider a serial mechanism having three compliant joints.*

(a) *A given compliance* $\mathbf{C}$ *can be realized with the mechanism if line* $l_1 \perp \mathbf{K}\mathbf{t}_1$ *is in the space spanned by joint twist* $\mathbf{t}_2$ *or* $\mathbf{t}_3$.
(b) *Every compliance matrix can be realized by the mechanism if and only if the union of spaces spanned by twists* $\mathbf{t}_2$ *and* $\mathbf{t}_3$ *is no less than a half plane.*

Proposition 4a provides a sufficient condition for a mechanism to realize a given compliance matrix. Since the invariant line $l_1 \perp \mathbf{K}\mathbf{t}_1$ is in the space spanned by $\mathbf{t}_2$ or $\mathbf{t}_3$, there exists a configuration at which l_1 is collinear with $\mathbf{t}_2$ or $\mathbf{t}_3$. Thus, the given compliance can be realized with two compliant joints J_1 and J_2, or J_1 and J_3, or all three joints.

For Proposition 4b, if the union of ranges of $\mathbf{t}_2$ and $\mathbf{t}_3$ continuously spans more than a half plane, then for any compliance, one of the two twists, $\mathbf{t}_2$ or $\mathbf{t}_3$, must be able to cross line $l_1 \perp \mathbf{K}\mathbf{t}_1$. On the other hand, if the union of spaces of $\mathbf{t}_2$ and $\mathbf{t}_3$ does not span a half space or more, all possible compliances $\mathbf{C}_i = c_i \mathbf{t}_i \mathbf{t}_i^{\mathrm{T}}$ will not fill the boundary of the PSD cone. Therefore, some endpoint compliances would not be able to be realized by the mechanism at the specified endpoint. Thus, Proposition 4b is a necessary and sufficient condition to realize all compliances at a given endpoint location with a given mechanism.

2.4 Joint Elasticity Compliance Realization Conditions. Equations used to calculate the set of joint compliance coefficients needed to realize a given compliance $\mathbf{C}$ were identified in Ref. [24] for 3R mechanisms at a given configuration (known joint locations described by $\mathbf{r}_i$). These equations can be equivalently expressed in terms of joint twists $\mathbf{t}_i$ using Eq. (3) and therefore generalized for use with all three-joint serial planar mechanisms.

Thus, for a given mechanism configuration with twists $\mathbf{t}_1$, $\mathbf{t}_2$, $\mathbf{t}_3$, and a realizable $\mathbf{C}$, the joint compliances are calculated using

$$c_1 = \frac{\mathbf{t}_2^{\mathrm{T}}(\Omega^{\mathrm{T}}\mathbf{C}\Omega)\mathbf{t}_3}{\mathbf{t}_2^{\mathrm{T}}\Omega^{\mathrm{T}}\mathbf{t}_1\mathbf{t}_1^{\mathrm{T}}\Omega\mathbf{t}_3} \tag{13}$$

$$c_2 = \frac{\mathbf{t}_3^{\mathrm{T}}(\Omega^{\mathrm{T}}\mathbf{C}\Omega)\mathbf{t}_1}{\mathbf{t}_3^{\mathrm{T}}\Omega^{\mathrm{T}}\mathbf{t}_2\mathbf{t}_2^{\mathrm{T}}\Omega\mathbf{t}_1} \tag{14}$$

$$c_3 = \frac{\mathbf{t}_1^{\mathrm{T}}(\Omega^{\mathrm{T}}\mathbf{C}\Omega)\mathbf{t}_2}{\mathbf{t}_1^{\mathrm{T}}\Omega^{\mathrm{T}}\mathbf{t}_3\mathbf{t}_3^{\mathrm{T}}\Omega\mathbf{t}_2} \tag{15}$$

Note that for a given configuration, the joint compliances are each unique. Also, it can be proved that, for a realizable $\mathbf{C}$, each c_i calculated by Eqs. (13)–(15) is non-negative.

2.5 Discussion. The theories presented in this section apply to each of the eight different three-joint mechanism topologies. The 3R case has previously been addressed using different methods [24]. Although described in different vector spaces ($\mathbf{r}_i$ vs. $\mathbf{t}_i$), the results are equivalent. In addition to developing these conditions for the 3R case, geometrical conditions for the realization of all compliant behaviors at a given endpoint location were also identified in Ref. [24]. Equivalent conditions are needed for the remaining three-joint kinematic topologies.

The 3P case is the easiest to address. Recall that, for a revolute joint J_i, the space spanned by the joint twist depends on the rotation range and the location of the joint; whereas, for a prismatic joint J_i, the joint twist depends only on the direction of the joint axis. Therefore, the space spanned by the joint twist depends on the rotation range of link-$(i-1)$ on which the prismatic joint is mounted. If all three joints are prismatic, the three twists are constant and independent of the mechanism configuration. Thus, a 3P mechanism cannot realize all compliances by changing its configuration. Therefore, to realize all compliance matrices with a serial mechanism, at least one joint in the mechanism must be revolute.

Conditions for the realization of all compliant behaviors at a given endpoint location for the remaining six kinematic topologies are addressed in Secs. 3 and 4. For each type of mechanism, the requirements on the twist space presented in Proposition 4 are interpreted in terms of kinematic conditions on the mechanism. Satisfaction of the identified conditions guarantees that all compliant behaviors can be achieved with the mechanism by properly selecting its configuration and each joint stiffness. Section 3 addresses three-joint mechanisms having one prismatic and two revolute joints, and the Sec. 4 addresses mechanisms having two prismatic and one revolute joints.

3 Mechanisms With One Prismatic and Two Revolute Joints

In this section, mechanisms having one prismatic joint and two revolute joints are considered. If the endpoint of the mechanism is specified, the mechanism is kinematically equivalent to a four-link mechanism. For each case, a necessary and sufficient condition is identified for the mechanism to realize every positive definite compliance matrix by varying just the mechanism configuration and the joint stiffness values. In each of the three kinematic topologies considered, it is assumed that the range of each joint separately is not restricted. Only joint limits based on kinematics are considered.

3.1 PRR Mechanisms. Consider the PRR mechanism shown in Fig. 5. The lengths of link-1, link-2, and link-3 are L_1, L_2, and L_3, respectively, and the perpendicular distance from endpoint O to the axis of prismatic joint J_1 is L_0.

Joint twist $\mathbf{t}_1$ is constant, whereas, the joint twists of J_2 and J_3, $\mathbf{t}_2$ and $\mathbf{t}_3$ (perpendicular to the position vectors $\mathbf{r}_2$ and $\mathbf{r}_3$) can change because the configuration can change. It can be seen that the range of $\mathbf{r}_2$ is within the range of $\mathbf{r}_3$ throughout the mechanism's range of motion. Thus, the space spanned by $\mathbf{t}_2$ is within the space spanned by $\mathbf{t}_3$.

As stated in Proposition 4b, in order to realize every compliance at a given endpoint O, the union of the space of twists spanned by $\mathbf{t}_2$ and $\mathbf{t}_3$ must be no less than a half plane. Therefore, to realize every compliant behavior at a given endpoint, only conditions on link lengths that ensure that the space spanned by $\mathbf{t}_3$ is more than a half plane are needed. Since $\mathbf{t}_3 \perp \mathbf{r}_3$, the necessary and sufficient condition for the mechanism to realize all compliances is that link-3 ($\mathbf{r}_3$) can rotate through more than 180 deg.

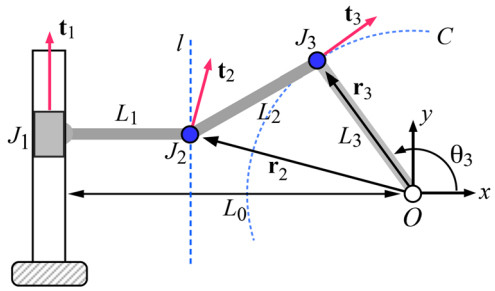

Fig. 5 Geometric parameters of a PRR mechanism. The locus of J_2 locations is line l, and the locus of J_3 locations is circle C.

Link-3 has four extreme positions as shown in Fig. 6. Two extreme positions occur when link-1 and link-2 are fully extended and collinear, which occur when J_3 is at the intersection of line l_1 and circle C, as shown in Fig. 6(*a*). The other two extreme positions occur when link-2 folds over link-1 and J_3 is at the intersection of line l_2 and circle C, as shown in Fig. 6(*b*). The two extreme angles are determined by

$$\cos\theta_{3m} = \frac{L_1 + L_2 - L_0}{L_3} \tag{16}$$

$$\cos\theta_{3M} = \frac{L_1 - L_2 - L_0}{L_3} \tag{17}$$

Thus, if solutions to both Eqs. (16) and (17) can be found, then link-3 rocks between $\cos\theta_{3m}$ and $\cos\theta_{3M}$ and its range of rotation is less than 180 deg.

It can be seen from Figs. 6(*a*) and 6(*b*) that the two extreme angles exist if and only if circle C intersects both lines l_1 and l_2. Thus, in order for the mechanism to realize all compliances, circle C must not intersect at least one of the two lines. Based on the relations of circle C with lines l_1 and l_2, the following cases are evaluated.

Case 1: Circle C intersects only line l_1. Then

$$L_0 + L_2 \geq L_1 + L_3$$

and θ_{3M} does not exist. Link-3 can rotate through $\theta_3 = 180$ deg to reach its reflection configuration $J'_1J'_2J'_3$ shown in Fig. 6(*a*). In order for link-3 to rotate more than 180 deg, θ_{3m} must be less than 90 deg. By Eq. (16), $L_1 + L_2 - L_0 \geq 0$. Thus,

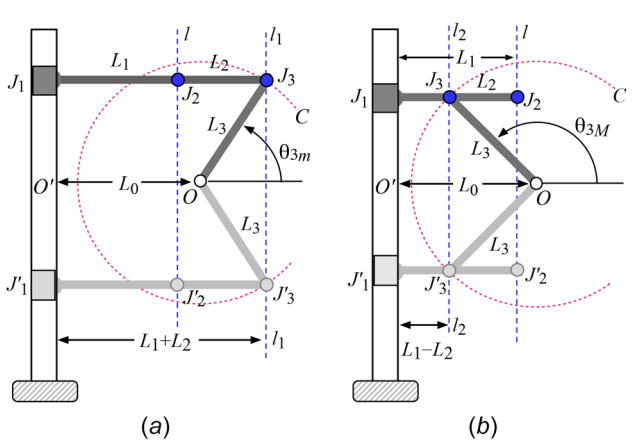

Fig. 6 Extreme positions of a PRR mechanism. The extreme positions of link-3 occur when link-2 is parallel to line OO'. (*a*) Link-1 and link-2 are collinear, and J_3 is at the intersection of line l_1 and circle C. (*b*) Link-2 folds over link-1, and J_3 is at the intersection of line l_2 and circle C.

$$L_1 - L_2 + L_3 \leq L_0 \leq L_1 + L_2 \tag{18}$$

Condition (18) is satisfied if l_1 is to the right of point O and l_2 is to the left of circle C.

Case 2: Circle C intersects only line l_2. Then

$$L_1 + L_2 \geq L_0 + L_3$$

and θ_{3m} does not exist. Link-3 can rotate through $\theta_3 = 0$ to reach its reflection configuration $J'_1J'_2J'_3$ shown in Fig. 6(*b*). In order for link-3 to rotate more than 180 deg, θ_{3M} must be greater than 90 deg. By Eq. (17), $L_0 - L_1 + L_2 \geq 0$. Thus,

$$L_1 - L_2 \leq L_0 \leq L_1 + L_2 - L_3 \tag{19}$$

Condition (19) is satisfied if l_1 is to the right of circle C and l_2 is to the left of point O.

Case 3: Circle C intersects neither l_1 nor l_2. If circle C is between lines l_1 and l_2, then, link-3 can make a full revolution and the mechanism can realize all compliances.

It is easy to verify that, for this case, both conditions (18) and (19) from case 1 and case 2 are satisfied. Thus, conditions (18) and (19) are necessary conditions for circle C to intersect neither l_1 nor l_2.

In summary, we have:

PROPOSITION 5. *For a PRR serial mechanism, any compliance can be realized if and only if condition (18) or (19) is satisfied.*

A PRR mechanism can realize all compliances if and only if the mechanism endpoint O is between lines l_1 and l_2 and circle C intersects the two lines at two or fewer points.

3.2 RPR Mechanisms. Consider the RPR mechanism with a specified endpoint O shown in Fig. 7. In this general RPR mechanism, the line of action of the prismatic joint does not necessarily pass through the revolute joint. This offset is illustrated here as the length of link-1, L_1, which is in general just the perpendicular distance from revolute joint J_1 to the prismatic axis along which joint J_3 is guided.

Note that twist $\mathbf{t}_2$ is along link AB and twist $\mathbf{t}_3$ is perpendicular to link-3 (OJ_3). To obtain the relationship between the twist spaces associated with prismatic joint J_2 and revolute joint J_3, consider the extreme positions of link-1. As shown in Fig. 8(*a*), at an extreme position of link-1, J_1A is parallel to link-3 (OJ_3). Therefore, the rotation range of link-1 (θ_1 in Fig. 7) is always within the rotation range of link-3 (θ_3 in Fig. 7). Since twist $\mathbf{t}_2 \perp J_1A$ and twist $\mathbf{t}_3 \perp OJ_3$, the space spanned by $\mathbf{t}_2$ is inside of the space spanned by $\mathbf{t}_3$. Therefore, the mechanism's ability to realize any compliance depends on the range of motion of link-3 and its extreme positions. Since the locus of point A locations is circle C_1 and the locus of joint J_3 locations is circle C_2 as shown in Fig. 8, the two cases considered below are based on the relations of the two circles.

Case 1: Circles C_1 and C_2 intersect at two points. As shown in Fig. 8(*b*), link-3 reaches an extreme position when joint J_3 is at

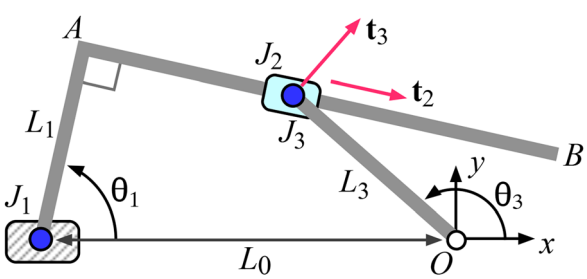

Fig. 7 Geometric parameters of an RPR mechanism. L_1 is the perpendicular distance from revolute joint J_1 to the axis along which joint J_3 is guided.

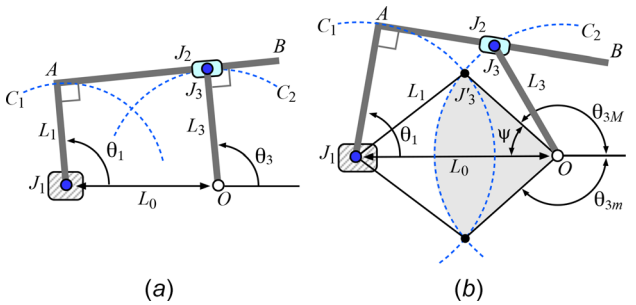

Fig. 8 Extreme positions of an RPR mechanism. (*a*) The extreme position of link-1 occurs when J_1A is parallel to link-3 (OJ_3). (*b*) The extreme position of link-3 occurs when J_3 is at the intersection point of circles C_1 and C_2. Link-3 cannot enter the interior of the shaded area.

one of the two intersection points of the two circles. Link-3 is not able to enter the shaded area of Fig. 8(*b*).

In order for link-3 to have a range greater than 180 deg, angle ψ in Fig. 8(*b*) must be less than 90 deg, which requires

$$L_0^2 + L_3^2 \geq L_1^2 \tag{20}$$

This condition ensures that any compliance can be realized with the mechanism.

Case 2: Circles C_1 and C_2 do not intersect. For this case, link-3 can make a full rotation.

If the two circles are separated, then the following condition must be satisfied:

$$L_1 + L_3 < L_0 \tag{21}$$

If one circle is completely inside of the other, then C_1 must be inside C_2, otherwise the desired endpoint location cannot be attained. The geometric condition for this case is

$$L_0 + L_1 < L_3 \tag{22}$$

It is easy to verify that if either condition (21) or (22) is satisfied, condition (20) must be satisfied.

In summary, we have:

PROPOSITION 6. *Any compliance can be realized with a serial RPR mechanism if and only if condition (20) is satisfied.*

For the special case in which the offset $L_1 = 0$, condition (20) is satisfied for all L_0 and L_3. Hence, all compliances can be realized by the mechanism.

3.3 RRP Mechanisms. Consider the general RRP serial mechanism shown in Fig. 9. The (perpendicular) distance from the mechanism endpoint O to the prismatic axis is L_3. In order to assess the mechanism ability to realize all compliances at a given location, only the twist spaces associated with joints J_2 and J_3 need to be considered.

As shown in Fig. 9, the twist associated with J_2 is perpendicular to $\mathbf{r}_2$, the position vector of J_2 relative to O. The twist associated with J_3 is along bar AB which is perpendicular to OA. Thus, the spaces spanned by $\mathbf{t}_2$ and $\mathbf{t}_3$ are determined by the rotation range of $\mathbf{r}_2$ and bar OA. The locus of J_2 locations is the circle C of radius L_1 centered at J_1. The locus of point A locations on link-3 is the circle C_O of radius L_3 centered at O. The locus of J_3 locations is bounded by circles C_1 and C_2 that are centered at J_1 having radiuses $(L_1 + L_2)$ and $(L_1 - L_2)$, respectively.

Because J_3 is a prismatic joint, the extreme positions of link-3 occur when J_3 is located on circle C_1 and when located on circle C_2. Figure 10 illustrates the two upper extreme positions of link-3. The other two extreme positions are symmetric to the upper ones below line OJ_1. At one extreme position, link-1 and link-2 are

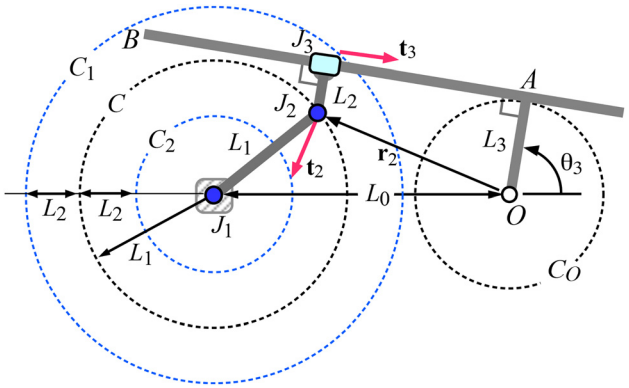

Fig. 9 Geometric parameters of an RRP mechanism. L_3 is the (perpendicular) distance from the mechanism endpoint O to the prismatic axis.

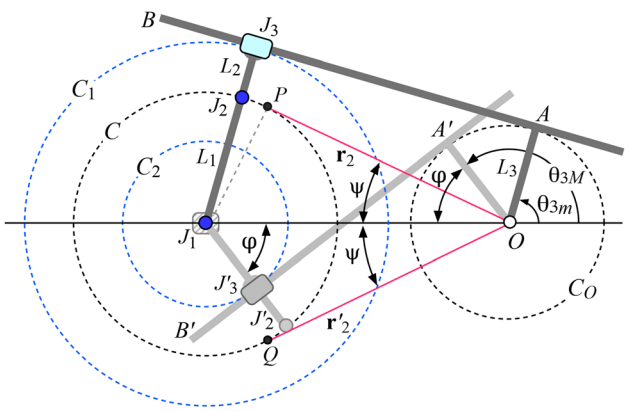

Fig. 10 Extreme positions of an RRP mechanism. The extreme position of link-3 occurs when prismatic joint J_3 reaches circles C_1 and C_2. When J_3 is on circle C_1, link-1 and link-2 are fully extended. When J_3 is on circle C_2, link-2 folds over link-1.

fully extended from base joint J_1, and bar AB is tangent to both circle C_O and circle C_1. At the other extreme position, link-2 folds over link-1 and bar AB is tangent to both circle C_O and circle C_2.

The two extreme angles θ_{3m} and θ_{3M} are determined by

$$\cos\theta_{3m} = \frac{L_1 + L_2 - L_3}{L_0} \tag{23}$$

$$\cos\theta_{3M} = -\frac{L_1 - L_2 + L_3}{L_0} \tag{24}$$

Based on the evaluations of θ_{3m} and θ_{3M}, the following cases are considered.

Case 1: Both extreme positions θ_{3m} and θ_{3M} exist. Bar OA of link-3 is able to rock between the two extreme positions, θ_{3m} and θ_{3M}. The conditions for this case are

$$\frac{|L_1 + L_2 - L_3|}{L_0} \leq 1, \quad \frac{|L_1 - L_2 + L_3|}{L_0} \leq 1$$

The above two inequalities are equivalent to

$$L_1 + |L_2 - L_3| \leq L_0 \tag{25}$$

Since link-3 rocks between the two extreme positions, it cannot rotate through more than 180 deg, and the space spanned by $\mathbf{t}_3$ alone will not be a half plane or more. Thus, the twist space associated with J_2 must be also considered. In order for the mechanism to realize all compliances, the union of the two twist spaces must

be more than a half plane. Since twist $\mathbf{t}_2 \perp \mathbf{r}_2$ and $\mathbf{t}_3 \perp OA$, the union of spaces spanned by $\mathbf{r}_2$ and OA must be more than a half plane.

As shown in Fig. 10, the space spanned by $\mathbf{r}_2$ is determined by the two lines OP and OQ both tangent to circle C. The space spanned by OA is determined by the two extreme positions of the bar (OA and OA' in Fig. 10). Thus, to obtain a large connected range of twists,

$$\varphi \le \psi, \quad \text{and} \quad \theta_{3m} \le \psi \tag{26}$$

The first inequality ensures that the two spaces spanned by $\mathbf{r}_2$ and OA are connected. The second inequality ensures that the union of the two spaces (bounded by the ray along OA at θ_{3m} and the ray OQ as shown in Fig. 10) is more than a half plane. To express the conditions in terms of link lengths, note that

$$\sin\psi = \frac{L_1}{L_0}, \quad \cos\varphi = \frac{L_1 - L_2 + L_3}{L_0}$$

and the two inequalities in Eq. (26) can then be written as

$$\sin\psi = \frac{L_1}{L_0} \ge \sin\varphi = \sqrt{1 - \frac{(L_1 - L_2 + L_3)^2}{L_0^2}}$$

$$\sin\psi = \frac{L_1}{L_0} \ge \sin\theta_{3m} = \sqrt{1 - \frac{(L_1 + L_2 - L_3)^2}{L_0^2}}$$

Solving the above equalities yields

$$|L_2 - L_3| \le L_1 - \sqrt{L_0^2 - L_1^2} \tag{27}$$

$$\text{or} \quad |L_2 - L_3| \ge L_1 + \sqrt{L_0^2 - L_1^2} \tag{28}$$

Since inequality (28) is not consistent with inequality (25), inequalities (25) and (27) are the conditions on the mechanism link lengths that ensure that all compliances can be realized. The two conditions can be written as

$$|L_2 - L_3| \le \min\left\{(L_0 - L_1), (L_1 - \sqrt{L_0^2 - L_1^2})\right\} \tag{29}$$

Thus, for case 1, condition (29) is a necessary and sufficient condition for the mechanism to realize all compliances at the given endpoint.

Case 2: One of the extreme positions θ_{3m} or θ_{3M} does not exist. For this case, inequality (25) is not satisfied. Thus,

$$|L_2 - L_3| > L_0 - L_1 \tag{30}$$

If θ_{3M} does not exist, as shown in Fig. 11(*a*), link-3 can rotate through $\theta_3 = 180$ deg from extreme position $J_1J_2J_3$ at $\theta_3 = \theta_{3m}$ to its reflection extreme position $J_1'J_2'J_3'$ at $\theta_3 = -\theta_{3m}$. Condition (30) ensures that $\theta_{3m} < 90$ deg, which means bar OA can rotate through more than 180 deg.

If θ_{3m} does not exist, as shown in Fig. 11(*b*), link-3 can rotate through $\theta_3 = 0$ from extreme position $J_1J_2J_3$ at $\theta_3 = \theta_{3m}$ to its reflection extreme position $J_1'J_2'J_3'$ at $\theta_3 = -\theta_{3m}$. Condition (30) ensures that $\theta_{3M} > 90$ deg, which means bar OA can rotate through more than 180 deg.

Thus, for case 2, all compliances can be realized.

In summary, we have:

PROPOSITION 7. *A serial RRP mechanism can realize all compliance matrices if and only if either condition (29) or (30) is satisfied.*

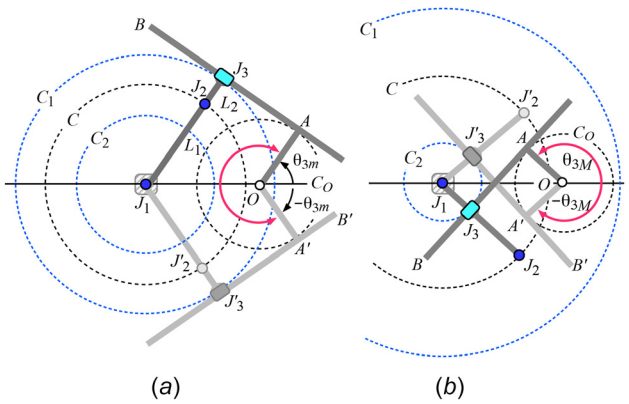

Fig. 11 Extreme positions of an RRP mechanism. (*a*) If θ_{3M} does not exist, link-3 can rotate through $\theta_3 = 180$ *deg* in going from position θ_{3m} to position $-\theta_{3m}$. (*b*) If θ_{3m} does not exist, link-3 can rotate through $\theta_3 = 0$ in going from position θ_{3M} to position $-\theta_{3M}$. For each case, prismatic joint J_3 will pass through point *A* of link *AB*.

Note that condition (29) requires that

$$0 \le \sqrt{L_0^2 - L_1^2} < L_1 < L_0$$

If $L_0 < L_1$, condition (30) is satisfied for all L_2 and L_3, and thus the mechanism can realize all compliances.

4 Mechanisms With One Revolute and Two Prismatic Joints

In this section, mechanisms having two prismatic joints and one revolute joint are considered. Unlike Sec. 3, some limits to the range of prismatic joints are assumed.

4.1 PPR Mechanisms. Consider the PPR mechanism shown in Fig. 12. The angle between the axes of the two prismatic joints is β. If there are no limits on the two prismatic joints, there are no extreme positions for link-3. Link-3 can make a full rotation, and thus any compliance can be realized with the mechanism.

If the ranges of joint-1 and link-2 are limited, the rotation range of link-3 may also be limited. If L_{im} and L_{iM} are the limits of prismatic joint J_i, then it is easy to verify that if

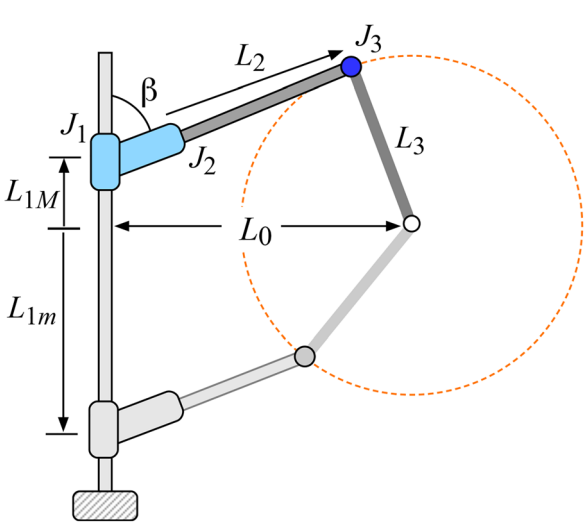

Fig. 12 Geometric parameters of a PPR mechanism. The motion of link-3 is restricted by the limits of the two prismatic joints.

$$L_3 \le \min\{(L_{1M} + L_{2M}\cos\beta), (L_{1m} - L_{2M}\cos\beta)\} \quad (31)$$

$$L_{2m}\sin\beta \le L_0 - L_3 \le L_0 + L_3 \le L_{2M}\sin\beta \quad (32)$$

the full rotation condition is satisfied. Thus, conditions (31) and (32) are sufficient conditions on the mechanism to have the ability to realize all compliances.

4.2 PRP Mechanisms. Consider the general PRP mechanism shown in Fig. 13. Note that joint J_2 moves along line l and point A moves along circle C of radius L_3 centered at O. The offset of prismatic joint J_3 from J_2 is illustrated here as the length of link-3, L_3, which is in general just the perpendicular distance from revolute joint J_2 to the prismatic axis.

There are two limiting positions of link OAB when bar OA is parallel to OO' ($\theta_3 = 0$ deg or 180 deg). For these two positions, J_1 is at infinity. Thus, OA cannot rotate more than 180 deg. In practice, the ranges of motion of J_2 and J_3 are limited by the limits of prismatic joint J_1 (L_{1M} and L_{1m}), as shown in Fig. 13.

Suppose θ_{3m} and θ_{3M} are the minimum and maximum angles of link-3 associated with L_{1M} and L_{1m}, respectively (shown in Fig. 13). In order to realize an arbitrary compliance, the space spanned by $\mathbf{t}_2$ and $\mathbf{t}_3$ together must be more than a half plane. It can be seen that the two joint twist spaces are connected. They span a half plane or more if and only if the angle φ in Fig. 13 satisfies $\varphi \ge \theta_{3m}$.

The equation for determining θ_{3m} (derived in the Appendix) is

$$L_{1M}\sin\theta_{3m} - (L_0 - L_2)\cos\theta_{3m} = L_4 - L_3 \quad (33)$$

The condition $\varphi \ge \theta_{3m}$ can be expressed in terms of the mechanism link lengths as

$$\frac{L_{1M}L_{1m} - (L_0 - L_2)^2}{(L_0 - L_2)(L_{1M} + L_{1m})} \ge \frac{L_4 - L_3}{\sqrt{L_{1M}^2 + (L_0 - L_2)^2 - (L_4 - L_3)^2}} \quad (34)$$

In summary, we have:

PROPOSITION 8. *Any compliance can be realized with a serial RPR mechanism if and only if condition (34) is satisfied.*

Note that condition (34) requires

$$L_{1M}^2 + (L_0 - L_2)^2 - (L_4 - L_3)^2 > 0$$

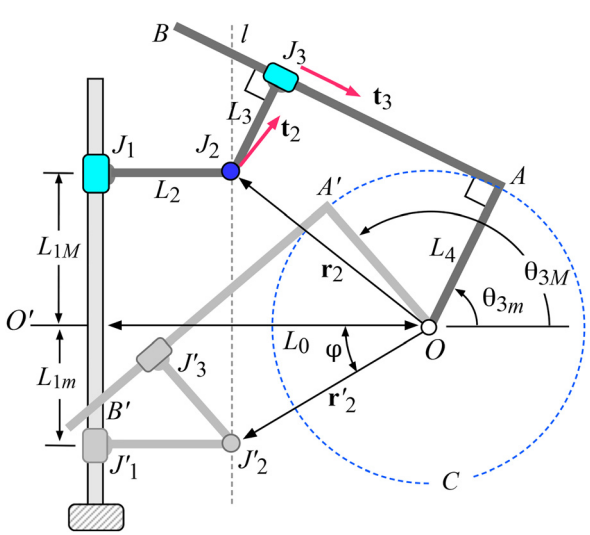

Fig. 13 Geometric parameters of a PRP mechanism. The extreme positions can be determined by the limits of J_1, L_{1M}, and L_{1m}.

If this inequality is not satisfied, the given endpoint location O cannot be attained.

If the offsets $L_3 = L_4 = 0$, condition (34) becomes

$$L_{1M}L_{1m} \ge (L_0 - L_2)^2$$

This condition indicates that, for $L_3 = L_4 = 0$, the mechanism can realize any compliance if and only if link-3 can rotate through more than 90 deg.

4.3 RPP Mechanisms. Consider the general RPP mechanism illustrated in Fig. 14. The angle between the axes of the two prismatic joints is β ($\beta \le 90$ deg). If the endpoint O is specified, the mechanism is kinematically equivalent to an RPPR mechanism. Similar to a PPR mechanism discussed in Sec. 4.1, if the prismatic joints are not limited, an RPP mechanism has no extreme positions and thus can realize all compliances.

If the ranges of the two prismatic joints are limited, the rotation range of link-3 may be constrained. Since the angle between the twists associated with the two prismatic joints is constant, the space spanned by the two twists is over a half plane if and only if link-3 (or joint-1) can rotate through more than $(180\,\text{deg} - \beta)$. Thus, for limited ranges of the two prismatic joints, the requirement for the mechanism to realize all compliances is that link-1 (or link-3) can rotate $(180\,\text{deg} - \beta)$ or more.

If the axes of the two prismatic joints are orthogonal ($\beta = 90$ deg), the requirement for the mechanism to realize all compliances is that link-1 can rotate 90 deg or more.

5 Compliance Synthesis

If a compliance is realizable at a given location with a given mechanism, a procedure to determine an appropriate configuration and associated joint compliance coefficients is needed.

Proposition 4 states that if a compliance $\mathbf{C}$ can be realized with a three-joint mechanism, $\mathbf{C}$ can always be realized with only two compliant joints, either J_1 and J_2 or J_1 and J_3, with the remaining joint having $c_i = 0$. Although loading all three joints with variable joint compliances is not necessary to realize a compliance, mechanisms with three compliant joints have the advantage that a significant amount of compliances can be reached with the mechanism by just changing the joint compliances while keeping the configuration unchanged.

In this section, two types of synthesis procedures for any given realizable compliance are provided. First, a synthesis procedure for the realization of a compliance using a three-joint mechanism having only two compliant joints is developed. Then, a synthesis procedure for the general case in which all three joints of a three-joint mechanism are compliant is presented. Examples are presented in Sec. 6.

5.1 Synthesis Procedure for Two Compliant Joints. For a mechanism in which only two of the three joints are compliant,

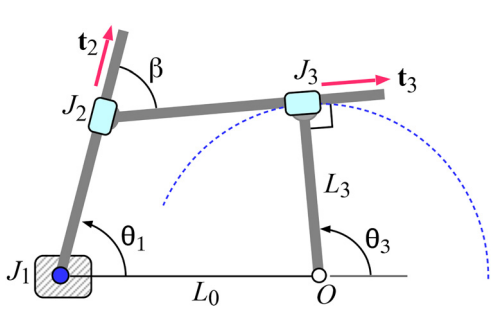

Fig. 14 An RPP mechanism. Link-1 and link-3 have the same range of rotation variation.

both the mechanism configuration and the joint compliances need to be changed, if the desired compliance is changed.

Below, a synthesis procedure is developed to realize an arbitrary compliance with a three-joint mechanism having compliance at two joints. For a given compliance $\mathbf{C}$, the procedure determines the mechanism configuration and joint compliances.

Consider a given three-joint mechanism. The distance between compliance frame origin O and the base joint J_1 is specified as L_0. If J_1 is a prismatic joint, L_0 is the perpendicular distance between O and the prismatic axis. The three-step synthesis procedure is:

(1) Determine joint twist $\mathbf{t}_1$ and determine the straight line $l_1 \perp \mathbf{Kt}_1$.
(2) Determine a mechanism configuration such that the joint twist $\mathbf{t}_2$ (or $\mathbf{t}_3$) is collinear to l_1.
(3) Determine the values of the joint compliance c_1 and c_2 (or, c_1 and c_3) using Eqs. (13)–(15).

With this procedure, the mechanism configuration and the joint compliances are determined. Note that there could be two different configurations that realize the same compliance $\mathbf{C}$.

5.2 Synthesis Procedure for Three Compliant Joints. The synthesis procedure is based on the procedure used for the two compliant joint case (described in Sec. 5.1).

The four-step synthesis procedure is:

(1) Calculate the vector $\mathbf{Kt}_1$ and determine line $l_1 \perp \mathbf{Kt}_1$.
(2) Choose a configuration S' that realizes the given compliance $\mathbf{C}$ with two compliant joints J_1 and J_2 (or J_3) using the process presented in Sec. 5.1.
(3) Choose a new configuration S to realize the compliance with three joints. The configuration can be found by the following:
   (a) Determine line $l_3' \perp \mathbf{Kt}_3'$ (or line $l_2' \perp \mathbf{Kt}_2'$) based on the configuration S' determined in step 2.
   (b) Change the configuration S' such that $\mathbf{t}_3$ (or $\mathbf{t}_2$) is in the zone bounded by l_1 and l_2' (or l_3'). This zone is identified using Proposition 3a.
(4) Determine the values of joint compliance at configuration S using Eqs. (13)–(15).

With this procedure, the configuration and the joint compliances of the mechanism are determined. Note that when configuration S is obtained in step 3, line $l_2 \perp \mathbf{Kt}_2$ needs to be constructed to confirm that $\mathbf{t}_3$ is between l_1 and l_2 and satisfies the condition in Proposition 3a. If the conditions are not satisfied, a new configuration S closer to S' should be selected. Also, note that the synthesis solution is not unique.

6 Examples

Two examples are provided to illustrate the synthesis procedures presented in Sec. 5. The compliance matrix to be realized in both examples is

$$\mathbf{C} = \begin{bmatrix} 2 & 1 \\ 1 & 4 \end{bmatrix}$$

The RRP manipulator to be used for the realization of $\mathbf{C}$ is shown in Fig. 15(*a*). The link lengths of the mechanism are given as: $L_1 = 3$, $L_2 = 0$, and $L_3 = 0$. The distance between the base joint J_1 and the compliance frame origin O is specified as $L_0 = 2$. Since $L_1 > L_0$, by the results presented in Sec. 3.3, any compliance can be realized by the manipulator at this endpoint location.

The synthesis of $\mathbf{C}$ with two compliant joints is first performed. Then, the synthesis of $\mathbf{C}$ using three compliant joints of the mechanism is presented.

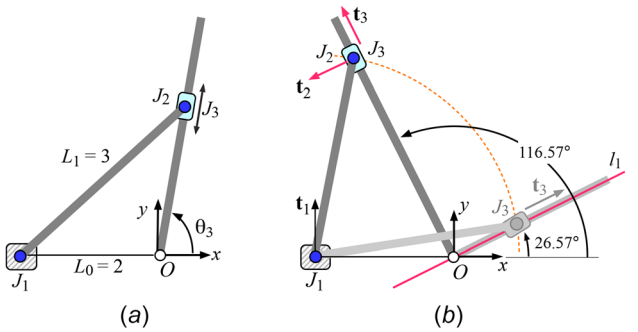

Fig. 15 (*a*) A specified RRP mechanism having given link length $L_1 = 3$. The position of joint base J_1 relative to the compliance frame origin O is specified $L_0 = 2$. (*b*) Configurations of the mechanism: Synthesis of $\mathbf{C}$ with two compliant joints J_1 and J_2 or J_1 and J_3.

6.1 Synthesis of C With Two Compliant Joints. The procedure presented in Sec. 5.1 is first used to synthesize compliance matrix $\mathbf{C}$.

Using the coordinate frame shown in Fig. 15, $\mathbf{t}_1$ and $\mathbf{Kt}_1$ are determined

$$\mathbf{t}_1 = \begin{bmatrix} 0 \\ -2 \end{bmatrix}, \quad \mathbf{Kt}_1 = \frac{1}{7}\begin{bmatrix} 2 \\ -4 \end{bmatrix}$$

Line $l_1 \perp \mathbf{Kt}_1$ (the angle between l_1 and the x-axis is 26.57 deg) and two configurations that satisfy the realization condition (5) are illustrated in Fig. 15(*b*). The darker configuration corresponds to having compliance in joints J_1 and J_2; whereas, the lighter configuration corresponds to having compliance in joints J_1 and J_3.

For the darker configuration, link-3 (OJ_3) is perpendicular to l_1 and $\mathbf{t}_2 \parallel l_1$. The three joint twists for this configuration are

$$\mathbf{t}_1 = \begin{bmatrix} 0 \\ -2 \end{bmatrix}, \quad \mathbf{t}_2 = \begin{bmatrix} 2.9541 \\ 1.4770 \end{bmatrix}, \quad \mathbf{t}_3 = \begin{bmatrix} -0.4472 \\ 0.8944 \end{bmatrix} \tag{35}$$

The values of joint compliances for the configuration calculated using Eqs. (13)–(15) are

$$c_1 = 0.8750, \quad c_2 = 0.2292, \quad c_3 = 0$$

For the lighter configuration, link-3 (OJ_3) is parallel to l_1 and $\mathbf{t}_3 \parallel l_1$. The three joint twists for this configuration are

$$\mathbf{t}_1 = \begin{bmatrix} 0 \\ -2 \end{bmatrix}, \quad \mathbf{t}_2 = \begin{bmatrix} -0.4806 \\ 0.9612 \end{bmatrix}, \quad \mathbf{t}_3 = \begin{bmatrix} 0.8944 \\ 0.4472 \end{bmatrix} \tag{36}$$

and the joint compliances calculated using Eqs. (13)–(15) are

$$c_1 = 0.8750, c_2 = 0, c_3 = 2.5000$$

In this example, two sets of configurations and compliant values are able to realize the specified compliance.

6.2 Synthesis of C With Three Compliant Joints. If compliance is provided in all three joints, the procedure presented in Sec. 5.2 is used to identify a mechanism configuration and associated joint compliances that will realize the compliance.

(1) Calculate $\mathbf{Kt}_1$ and determine line $l_1 \perp \mathbf{Kt}_1$, as described in Sec. 6.1.
(2) Choose a configuration S' that realizes the given compliance $\mathbf{C}$ with two compliant joints J_1 and J_2 (or J_1 and J_3). The three joint twists given in Eq. (35) are selected for this

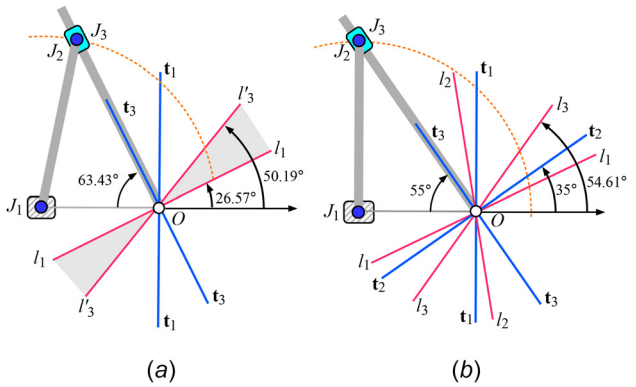

Fig. 16 Realization of the example compliance with three compliant joints. (*a*) Mechanism configuration associated with the realization using two compliant joints J_1 and J_2 is used to estimate the acceptable zone for $\mathbf{t}_2$. (*b*) Mechanism configuration associated with the realization using three compliant joints.

example as $\mathbf{t}'_1$, $\mathbf{t}'_2$, and $\mathbf{t}'_3$ (the joint twists in Eq. (36) could alternately be selected).

(3) Choose a new configuration S to realize the compliance with three joints.
   (a) Line $l'_3 \perp \mathbf{K}\mathbf{t}'_3$ is determined and is shown in Fig. 16(*a*). The angle between l'_3 and the x-axis is 50.19 deg. The estimated acceptable zone for $\mathbf{t}_2$ is the shaded area between l_1 and l'_3.
   (b) Choose a new configuration such that $\mathbf{t}_2$ is in the shaded area of Fig. 16(*a*). Here, $\mathbf{t}_2$ with an angle of 35 deg relative to x-axis is chosen. Once $\mathbf{t}_2$ is determined, $\mathbf{t}_3$ is calculated using mechanism kinematics. The three twists at this configuration are

$$\mathbf{t}_1 = \begin{bmatrix} 0 \\ -2 \end{bmatrix}, \quad \mathbf{t}_2 = \begin{bmatrix} 2.9984 \\ 2.0995 \end{bmatrix}, \quad \mathbf{t}_3 = \begin{bmatrix} -0.5736 \\ 0.8192 \end{bmatrix}$$

(4) Determine the values of joint compliance at configuration S using Eqs. (13)–(15), which for this case are

$$c_1 = 0.680, \quad c_2 = 0.2015, \quad c_3 = 0.5719$$

With this procedure, the mechanism configuration (shown in Fig. 16(*b*)) and the joint compliances are obtained. To confirm that the mechanism configuration satisfies the realization conditions, line $l_2 \perp \mathbf{K}\mathbf{t}_2$ and line $l_3 \perp \mathbf{K}\mathbf{t}_3$ corresponding to the final configuration are also illustrated in Fig. 16(*b*).

Note that, when synthesizing a given compliance with two compliant joints J_1 and J_2, there are two configurations each having a unique set of joint compliances; when synthesizing a given compliance with three compliant joints, there are an infinite number of configurations and sets of joint compliances for the given mechanism that realize the same compliance.

7 Summary

In this paper, methods to realize an arbitrary 2×2 elastic behavior using three-joint serial mechanisms are presented. The ability of any specified three-joint mechanism to realize an arbitrary compliance behavior is characterized. It is shown that if a mechanism has appropriately sized relative link lengths or joint range limits, every compliance matrix can be realized by the mechanism at the specified endpoint location. This ability allows the realization of *all* particle compliant behaviors with a *single* three-joint mechanism by properly selecting the joint compliances and the mechanism configuration.

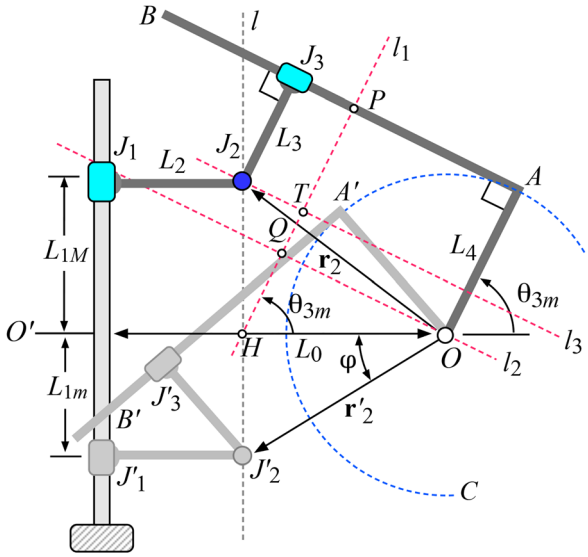

Fig. 17 Extreme positions of a PRP mechanism. The minimum angle of link-3 is determined by the upper limit of link-1, L_{1M}.

Acknowledgment

This work was supported by the National Science Foundation under Grant No. IIS-1427329.

Appendix

For the PRP mechanism shown in Fig. 13, the minimum angle of link-3, θ_{3m}, occurs when link-1 reaches its upper limit L_{1M}. To determine θ_{3m}, consider three lines l_1, l_2, and l_3 shown in Fig. 17. Line l_1 is parallel to bar OA and passes through point H, the intersection of line l and line OO'. Line l_2 is parallel to bar AB and passes through point O. Line L_3 is parallel to AB and passes through joint J_2. Then,

$$|HP| = |HQ| + |QP| = |HT| + |TP|$$

Since

$$|TP| = L_3, |HT| = L_{1M} \sin\theta_{3m}$$

$$|QP| = L_4, |HQ| = |HO| \cos\theta_{3m} = (L_0 - L_2)\cos\theta_{3m}$$

the following relationship holds:

$$L_{1M} \sin\theta_{3m} + L_3 = (L_0 - L_2)\cos\theta_{3m} + L_4$$

which proves Eq. (33).

Dividing Eq. (33) by $\sqrt{(L_0 - L_2)^2 + L_{1M}^2}$ yields

$$\frac{L_{1M}}{\sqrt{(L_0 - L_2)^2 + L_{1M}^2}} \sin\theta_{3m} - \frac{(L_0 - L_2)}{\sqrt{(L_0 - L_2)^2 + L_{1M}^2}} \cos\theta_{3m} = \frac{L_4 - L_3}{\sqrt{(L_0 - L_2)^2 + L_{1M}^2}}$$

which can be further simplified to

$$\sin(\theta_{3m} - \gamma) = \frac{L_4 - L_3}{\sqrt{(L_0 - L_2)^2 + L_{1M}^2}}$$

where

$$\gamma = \tan^{-1}\frac{(L_0 - L_2)}{L_{1M}}$$

The angle φ (shown in Fig. 17) associated with the lower limit of J_1, L_{1m}, can be obtained by

$$\tan\varphi = \frac{|HJ_2'|}{|HO|} = \frac{L_{1m}}{L_0 - L_2}$$

Then,

$$\tan(\varphi - \gamma) = \frac{\tan\varphi - \tan\gamma}{1 + \tan\varphi\tan\gamma} = \frac{L_{1M}L_{1m} - (L_0 - L_2)^2}{(L_{1M} + L_{1m})(L_0 - L_2)}$$

and

$$\begin{aligned}\tan(\theta_{3m} - \gamma) &= \frac{\sin(\theta_{3m} - \gamma)}{\sqrt{1 - \sin^2(\theta_{3m} - \gamma)}} \\ &= \frac{L_4 - L_3}{\sqrt{L_{1M}^2 + (L_0 - L_2)^2 - (L_4 - L_3)^2}}\end{aligned}$$

The condition $\varphi \geq \theta_{3m}$ is equivalent to

$$(\varphi - \gamma) \geq (\theta_{3m} - \gamma) \iff \tan(\varphi - \gamma) \geq \tan(\theta_{3m} - \gamma)$$

Thus,

$$\frac{L_{1M}L_{1m} - (L_0 - L_2)^2}{(L_0 - L_2)(L_{1M} + L_{1m})} \geq \frac{L_4 - L_3}{\sqrt{L_{1M}^2 + (L_0 - L_2)^2 - (L_4 - L_3)^2}}$$

References

[1] Albu-Schaffer, A., Eiberger, O., Grebenstein, M., Haddadin, S., Ott, C., Wimbock, T., Wolf, S., and Hirzinge, G., 2008, "Soft Robotics: From Torque Feedback-Controlled Lightweight Robots to Intrinsically Compliant Systems," IEEE Rob. Autom. Mag., **15**(3), pp. 20–30.

[2] Ham, R. V., Sugar, T. G., Vanderborght, B., Hollander, K. W., and Lefeber, D., 2009, "Compliant Actuator Designs," IEEE Rob. Autom. Mag., **16**(3), pp. 81–94.

[3] Pratt, G., and Williamson, M., 1995, "Series Elastic Actuators," 1995 IEEE/RSJ International Conference on Intelligent Robots and Systems, Aug. 5–9, Vol. 1, pp. 399–406.

[4] Ham, R. V., Sugar, T. G., Vanderborght, B., Hollander, K. W., and Lefeber, D., 2009, "Compliant Actuator Designs: Review of Actuators With Passive Adjustable Compliance/Controllable Stiffness for Robotic Applications," IEEE Rob. Autom. Mag., **16**(3), pp. 81–94.

[5] Ball, R. S., 1900, *A Treatise on the Theory of Screws*, Cambridge University Press, London, UK.

[6] Dimentberg, F. M., 1965, "The Screw Calculus and Its Applications in Mechanics," Foreign Technology Division, Wright-Patterson Air Force Base, Dayton, OH, Document No. FTD-HT-23-1632-67.

[7] Griffis, M., and Duffy, J., 1991, "Kinestatic Control: A Novel Theory for Simultaneously Regulating Force and Displacement," ASME J. Mech. Des., **113**(4), pp. 508–515.

[8] Patterson, T., and Lipkin, H., 1993, "Structure of Robot Compliance," ASME J. Mech. Des., **115**(3), pp. 576–580.

[9] Patterson, T., and Lipkin, H., 1993, "A Classification of Robot Compliance," ASME J. Mech. Des., **115**(3), pp. 581–584.

[10] Loncaric, J., 1987, "Normal Forms of Stiffness and Compliance Matrices," IEEE J. Rob. Autom., **3**(6), pp. 567–572.

[11] Huang, S., and Schimmels, J. M., 1998, "The Bounds and Realization of Spatial Stiffnesses Achieved With Simple Springs Connected in Parallel," IEEE Trans. Rob. Autom., **14**(3), pp. 466–475.

[12] Huang, S., and Schimmels, J. M., 2000, "The Bounds and Realization of Spatial Compliances Achieved With Simple Serial Elastic Mechanisms," IEEE Trans. Rob. Autom., **16**(1), pp. 99–103.

[13] Roberts, R. G., 1999, "Minimal Realization of a Spatial Stiffness Matrix With Simple Springs Connected in Parallel," IEEE Trans. Rob. Autom., **15**(5), pp. 953–958.

[14] Ciblak, N., and Lipkin, H., 1999, "Synthesis of Cartesian Stiffness for Robotic Applications," IEEE International Conference on Robotics and Automation, May 10–15, pp. 2147–2152.

[15] Huang, S., and Schimmels, J. M., 1998, "Achieving an Arbitrary Spatial Stiffness With Springs Connected in Parallel," ASME J. Mech. Des., **120**(4), pp. 520–526.

[16] Huang, S., and Schimmels, J. M., 2000, "The Eigenscrew Decomposition of Spatial Stiffness Matrices," IEEE Trans. Rob. Autom., **16**(2), pp. 146–156.

[17] Huang, S., and Schimmels, J. M., 2001, "A Classification of Spatial Stiffness Based on the Degree of Translational–Rotational Coupling," ASME J. Mech. Des., **123**(3), pp. 353–358.

[18] Roberts, R. G., 2000, "Minimal Realization of an Arbitrary Spatial Stiffness Matrix With a Parallel Connection of Simple Springs and Complex Springs," IEEE Trans. Rob. Autom., **16**(5), pp. 603–608.

[19] Choi, K., Jiang, S., and Li, Z., 2002, "Spatial Stiffness Realization With Parallel Springs Using Geometric Parameters," IEEE Trans. Rob. Autom., **18**(3), pp. 264–284.

[20] Petit, F. P., 2014, "Analysis and Control of Variable Stiffness Robots," Ph.D. thesis, ETH Zurich, Zurich, Switzerland.

[21] Belfiore, N. P., Verotti, M., Giamberardino, P. D., and Rudas, I. J., 2012, "Active Joint Stiffness Regulation to Achieve Isotropic Compliance in the Euclidean Space," ASME J. Mech. Rob., **4**(4), p. 041010.

[22] Verotti, M., and Belfiore, N. P., 2016, "Isotropic Compliance in E(3): Feasibility and Workspace Mapping," ASME J. Mech. Rob., **8**(6), p. 061005.

[23] Verotti, M., Masarati, P., Morandini, M., and Belfiore, N., 2016, "Isotropic Compliance in the Special Euclidean Group SE(3)," Mech. Mach. Theory, **98**, pp. 263–281.

[24] Huang, S., and Schimmels, J. M., 2016, "Realization of Point Planar Elastic Behaviors Using Revolute Joint Serial Mechanisms Having Specified Link Lengths," Mech. Mach. Theory, **103**, pp. 1–20.

[25] Albu-Schaffer, A., Fischer, M., Schreiber, G., Schoeppe, F., and Hirzinger, G., 2004, "Soft Robotics: What Cartesian Stiffness Can We Obtain With Passively Compliant, Uncoupled Joints?," 2004 IEEE/RSJ International Conference on Intelligent Robots and Systems, Sept. 28–Oct. 2, pp. 3295–3301.

[26] Huang, S., and Schimmels, J. M., 2002, "The Duality in Spatial Stiffness and Compliance as Realized in Parallel and Serial Elastic Mechanisms," ASME J. Dyn. Syst., Meas., Control, **124**(1), pp. 76–84.